Article

Investigation of the Relationship Between H2O2 and HClO in Living Cells by a Bifunctional, Dual-ratiometric Responsive Fluorescent Probe

Jinliang Han, Xingjiang Liu, Haiqing Xiong, Jingpei Wang, Benhua Wang, Xiangzhi Song, and Wei Wang

Anal. Chem., **Just Accepted Manuscript** • DOI: 10.1021/acs.analchem.9b05604 • Publication Date (Web): 03 Mar 2020

Investigation of the Relationship Between H_2O_2 and HClO in Living Cells by a Bifunctional, Dual-ratiometric Responsive Fluorescent Probe

Jinliang Han,[†] Xingjiang Liu,[‡] Haiqing Xiong,[†] Jingpei Wang,[†] Benhua Wang,[†] Xiangzhi Song,[†,*] and Wei Wang[≠,*]

[†] College of Chemistry & Chemical Engineering, Central South University, Changsha 410083, Hunan Province, China. Email: xzsong@csu.edu.cn.
[‡] College of Chemistry and Molecular Engineering, Zhengzhou University, Zhengzhou 450001, Henan Province, China.
[≠] Department of Pharmacology and Toxicology, College of Pharmacy, and BIO5 Institute, University of Arizona, Tucson, AZ, 85721, USA. Email: wwang@pharmacy.arizona.edu.

The corresponding author's full contact information: Prof. Wei Wang, PhD, Department of Pharmacology and Toxicology, College of Pharmacy, and BIO5 Institute, University of Arizona, 1703 E. Mabel Street, Tucson, AZ 85721-0207, USA. Email: wwang@pharmacy.arizona.edu; phone: 1-520-626-1764.

ABSTRACT: As two important reactive oxygen species (ROS), hydrogen peroxide (H_2O_2) and hypochlorous acid (HClO) play vital roles in many physiological and pathological processes. However, the relationship between these two species is seldomly investigated, in part, because of the lack of robust molecular tools which can simultaneously visualize HClO and H_2O_2 in biosystems. In this work, we present a design strategy to construct a single fluorescent probe that can detect H_2O_2 and HClO by simultaneously monitoring two distinct detection channels. In the design, one phenothiazine-based coumarin serves as a chromophore and sensor for HClO while a second coumarin precursor containing a boronate ester acts as a sensor for H_2O_2. After a head-to-head screening of three candidates differing in their coumarin precursor moieties, probe **CSU1** was found to have the optimal characteristics. As shown experimentally, it is able to detect them selectively and sensitively to generate distinct fluorescence signals and patterns in living cells. Furthermore, the endogenous generation of HClO from H_2O_2 and Cl^- catalyzed by MPO (myeloperoxidase) enzyme in living cells can be clearly monitored by the probe. These studies demonstrate the potential of the probe as a powerful tool to investigate the interplay of HClO and H_2O_2 in oxidative stress.

As the important species within and between cells, reactive oxygen species (ROS), such as $O_2^{-\bullet}$, $^\bullet OH$, $^1O_2$, HClO and H_2O_2, play vital roles in cell signal transmission, differentiation, migration, cellular immunity and body's defense against pathogens.[1-6] H_2O_2, as the most described signaling molecule among ROS families, is relatively stable and has various indispensable functions in cell signal transduction and homeostasis.[7-9] H_2O_2 is a precursor and a by-product in ROS chain reactions, and its excessive production can lead to oxidative damage and thereby cause aging and various diseases including cardiovascular diseases,[10] neurodegenerative diseases,[11] inflammation,[12] cancer,[13] *etc*.[14-16] Strong oxidant HClO is a microbicidal effector to cope with microbial invasion in immune system.[17,18] The abnormal accumulation of HClO can cause serious tissue damage[19] to induce a series of diseases including neurodegenerative diseases, atherosclerosis, cancer, ischemia, reperfusion injury, rheumatoid rheumatism, and so on.[20-24] In many cases, the delicate balance between oxidative stress and signal transduction in cells is strictly manipulated by a group of reactive oxygen species, which are mutually dependent and are often transformed into each other through intracellular reactions.[25] Since ROS are very reactive and their intracellular concentrations vary greatly, particularly in physiological and pathological conditions,[4] the simultaneous investigation of the activity of multiple ROS in cells is critically important to help study their interactions and synergistic effects in complex environments. For example, HClO can be endogenously produced from H_2O_2 and chloride ion with the catalysation of the myeloperoxidase enzyme (MPO) in leukocytes.[26, 27] In organisms, the levels of HClO and H_2O_2 are within a well specified range in order to maintain a relative balance. Once the balance is disrupted, oxidative stress occurs and thereby leading to aging and subsequent diseases such as neurodegenerative Alzheimer's and Parkinson's diseases.[28-30] As a result, the imaging tools capable of simultaneous detection of HClO and H_2O_2 are highly valued and urgently needed.

Fluorescence imaging technique offers a high spatial and temporal resolution and serves as an attractive tool to study biological species in a noninvasive manner.[31] Although numerous fluorescent probes have been developed for the single and specific detection of HClO or H_2O_2,[4, 32-40] as far as we are aware, there is no such probe that can simultaneously image both HClO and H_2O_2 *in vitro* and *in vivo*, especially in a ratiometric manner. Ratiometric fluorescent probes are more desirable because they can reduce the interference from the concentration of fluorescent probes, the instrument factor and the

environments through self-calibration with two fluorescence signals.[41] In light of the important roles that H_2O_2 and HClO play in biosystems, it would be of high interest in a probe that can simultaneously detect HClO and H_2O_2 with distinct signals.

Here, through the delicate design and after a head-to-head screening of three candidates, we obtain a dual-ratiometric fluorescent probe, **CSU1**, that can simultaneously detect H_2O_2 and HClO from different channels (see its structure in Scheme 1 and working mechanism in Scheme 2). With the aid of confocal microscope, this probe enables to image HClO and H_2O_2 in living cells, and particularly to observe the intracellular generation of HClO from H_2O_2 and Cl^- under the enzyme catalysation by virtue of ratiometric fluorescence changes.

EXPERIMENTAL SECTION

Materials and Instruments. The commercial chemicals were used without further purification. The organic solvents are analytically pure. NaClO was used as the source of HClO. ^1H and ^{13}C NMR spectra were obtained using a Bruker 400 spectrometer with chemical shifts reported in ppm (TMS as an internal standard). Mass spectra were obtained on a Bruker Daltonics micr-OTOF-Q II mass spectrometer. Emission spectra were recorded on a Hitachi F-7000 fluorometer, and UV-vis absorption spectra were recorded on an Agilent UV-2450 spectrophotometer. A Leici PHS-3C meter was used for pH measurements. The bioimaging experiments were carried out on an Opera Phenix/Operetta CLS system from Perkin Elmer and the analysis software was Harmony 4.5. Blue channel: 420-500 nm (excited at 355-385 nm); green channel: 515-580 nm (excited at 390-420 nm); red channel: 570-650 nm (excited at 435-460 nm). MCF-7 cells were provided by the State Key Laboratory of Chemo/Biosensing and Chemometrics, Hunan University, China.

Spectral Measurements. All the optical experiments except pH measurements were performed in PBS buffer (10.0 mM, pH 7.4, containing 50% acetonitrile). The stock solutions of fluorescent probes **(CSU1**, **CSU2** and **CSU3** in Scheme 1) (0.1 mM) were prepared in acetonitrile (CH_3CN). The solutions of various testing species stock solutions (10.0 mM) were prepared in twice-distilled water according to the literature methods (seen in ESI). For the titration experiments, a certain amount of H_2O_2 or HClO was added into the solution of a probe (5.0 μM) in a 2.0 mL total volume. The resulting solutions were shaken well and then incubated for 20 min at 25 °C before the spectral measurements.

Cell Culture. DMEM was added with 10% fetal bovine serum, 1% penicillin and 1% streptomycin as the culture medium, and cells were placed in the medium at 37 °C under a humidified atmosphere containing 5% CO_2 and 95% air. Before imaging experiments, cells were cultured in an 18 mm glass dish.

Cytotoxicity Assay. MTT assay was performed using MCF-7 cells, which were placed into 96-well plate and cultured in a cell culture tank. After the cell attachment was completed, different concentrations (0.0, 5.0, 10.0, 15.0, 20.0 μM) of probe **CSU1** were added into cells in 96-well plate, which were then incubated in 5% CO_2 humidified incubator for 24 h. The MTT solution (1.0 mg/mL in PBS buffer) was then added to each well and cells were incubated in a cell culture tank for another 4 h. Finally, the MTT solutions were dumped and DMSO (100.0 μL) was added to each well. The absorbance of DMSO solutions at 490 nm was determined and the cell viability was calculated using the following formula: cell viability = (mean absorbance of test wells - mean absorbance of medium control wells)/(mean absorbance of untreated wells - mean absorbance of medium control wells) × 100%.

Imaging of Exogenous H_2O_2 and HClO in MCF-7 Cells. MCF-7 cells were treated with probe **CSU1** (5.0 μM) for 20 min. Then **CSU1**-loaded MCF-7 cells were incubated with H_2O_2 (500.0 μM) for 60 min and HClO (400.0 μM) for 20 min, respectively. Cells were washed with PBS buffer three times before fluorescence imaging. For the successive imaging of exogenous H_2O_2 and HClO, **CSU1**-loaded cells were first incubated with H_2O_2 (500.0 μM) for 60 min, washed with PBS buffer three times, further treated with HClO (400.0 μM) for another 20 min, and finally washed with PBS buffer three times. A same procedure was use for the reverse addition order (from H_2O_2 to HClO).

General Procedure for Monitoring HClO Generation from H_2O_2 and Cl^- Induced by Myeloperoxidase (MPO) in Solution and Living Cells. First, the measurement of MPO-induced HClO from H_2O_2 and Cl^- was carried out in PBS buffer (10.0 mM, pH 7.4, containing 50% CH_3CN). Probe **CSU1** (5.0 μM), MPO (0.5 U/mL), NaCl (2.0 mM) and H_2O_2 (500.0 μM) were dissolved in the test solution. The mixture was incubated at 37 °C for a total 27 min during which the fluorescence intensity at respective 409 nm and 520 nm was measured every 3 min. For monitoring intracellular MPO-induced HClO from H_2O_2 and Cl^-, cells were first treated with probe **CSU1** (5.0 μM), NaCl (2.0 mM) and MPO (0.5 U/mL) for 20 min and then incubated with H_2O_2 (500.0 μM) for another 30 min at 37 °C. For the real-time monitoring the process of the endogenous HClO generation from H_2O_2 and Cl^- in the presence of MPO enzyme in living cells, cells was were treated with probe **CSU1** (5.0 μM), NaCl (2.0 mM) and MPO (0.5 U/mL) for 20 min, washed with PBS buffer three times and then observed under a microscope after the addition of H_2O_2 (500.0 μM) at 37 °C.

Synthesis of Compounds 1, 2 and 5. Compounds **1**, **2** and **5** were synthesized according to the reported methods (Scheme 1).[42-44]

Synthesis of Compound 3. To a solution of compound **2** (790 mg, 2.0 mmol) in 20 mL of MeOH was added NaOH (240 mg, 6.0 mmol). The reaction mixture was refluxed for 1 h. After removal of the solvent under a reduced pressure, the residue was dissolved in CH_2Cl_2 (50 mL) and acidified to pH 3.0-4.0 using 10% aqueous HCl solution, and then washed with water and brine. The organic layer was dried over anhydrous sodium sulfate and concentrated in vacuum to give a pure oxblood solid (672 mg, 91%). HRMS (ESI) m/z calcd for $C_{20}H_{17}NO_4S$ $[M+Na]^+$: 390.0776; found 390.0784. ^1H NMR (400 MHz, $CDCl_3$) δ 8.67 (s, 1H), 7.29 (s, 1H), 7.21 (t, J = 7.7 Hz, 1H), 7.11 (d, J = 7.5 Hz, 1H), 7.03 (t, J = 7.5 Hz, 1H), 6.94 (d, J = 8.2 Hz, 1H), 6.77 (s, 1H), 3.91 (t, J = 7.3 Hz, 2H), 1.88–1.76 (m, 2H), 1.51 (m, 2H), 0.99 (t, J = 7.3 Hz, 3H). ^{13}C NMR (100 MHz, $CDCl_3$) δ 164.6, 163.4, 156.3, 152.2, 149.7, 141.6, 128.0, 127.6, 126.7, 124.576, 122.9, 122.6, 116.5, 113.4, 109.9, 101.9, 48.6, 28.4, 20.1, 13.7.

Synthesis of Compounds SAB1-3. Compound **SA1** (152 mg, 1.0 mmol), 4-bromomethylphenylboronic acid pinacol ester (296 mg, 1.0 mmol), and K_2CO_3 (414 mg, 3.0 mmol) were placed in anhydrous CH_3CN (10.0 mL) under an argon atmosphere. The reaction mixture was refluxed for 5 h. After cooling to room temperature, 40 mL of water was added to the

mixture, which was extracted with 30.0 mL CH_2Cl_2 three times. The combined organic layers were dried over Na_2SO_4, and the solvent was evaporated under a reduced pressure. The crude product was chromatographed on silica gel flash column (300-400 mesh; eluent, petroleum ether (PE) : ethyl acetate (EA) = 5:1) to give **SAB1** as a white solid (312 mg, 85%). HRMS (ESI) m/z calcd for $C_{21}H_{25}BO_5$ $[M+Na]^+$: 391.1687; found 391.1704. ^{1}H NMR (400 MHz, $CDCl_3$) δ 10.39 (s, 1H), 7.84 (d, J = 9.9 Hz, 3H), 7.44 (d, J = 7.8 Hz, 2H), 6.55 (dd, J = 8.7, 1.4 Hz, 1H), 6.48 (d, J = 1.8 Hz, 1H), 5.18 (s, 2H), 3.83 (s, 3H), 1.35 (s, 12H). ^{13}C NMR (100 MHz, $CDCl_3$) δ 188.3, 166.1, 162.7, 139.0, 135.2, 130.5, 126.4, 119.3, 106.2, 99.2, 83.9, 70.3, 55.7, 24.9.

SAB2 was prepared in a similar procedure as a white solid (322 mg, 83% yield). HRMS (ESI) m/z calcd for $C_{24}H_{25}BNO_4$ $[M+Na]^+$: 411.1738; found 411.1729. ^{1}H NMR (400 MHz, $CDCl_3$) δ 10.99 (s, 1H), 9.29 (d, J = 8.5 Hz, 1H), 8.01 (d, J = 8.9 Hz, 1H), 7.85 (d, J = 7.6 Hz, 2H), 7.75 (s, 1H), 7.62 (t, J = 7.1 Hz, 1H), 7.44 (dd, J = 17.0, 7.5 Hz, 3H), 7.30 (d, J = 9.0 Hz, 1H), 5.36 (s, 2H), 1.35 (s, 12H). ^{13}C NMR (100 MHz, $CDCl_3$) δ 192.2, 163.2, 139.0, 137.6, 135.3, 131.6, 130.0, 128.7, 128.3, 126.5, 126.4, 125.0, 125.0, 113.9, 109.5, 84.0, 71.4, 24.9.

SAB3 was prepared in a similar procedure as a white solid (315 mg, 82% yield). HRMS (ESI) m/z calcd for $C_{20}H_{23}BO_4$ $[M+Na]^+$: 361.1582; found 351.1563. ^{1}H NMR (400 MHz, $CDCl_3$) δ 10.57 (s, 1H), 7.85 (dd, *J* = 7.6, 3.8 Hz, 3H), 7.51 (dd, *J* = 11.3, 4.4 Hz, 1H), 7.44 (d, *J* = 7.8 Hz, 2H), 7.07-6.96 (m, 2H), 5.22 (s, 2H), 1.35 (s, 12H). ^{13}C NMR (100 MHz, $CDCl_3$) δ 189.8, 161.0, 139.1, 135.9, 135.2, 128.5, 126.4, 125.2, 121.1, 113.0, 83.9, 70.4, 24.9.

Synthesis of Compounds SABC1-3. To a solution of compounds **SAB1** (128 mg, 0.4 mmol) and compound **5** (65 mg, 0.5 mmol) in ethanol (4.0 mL) was added piperidine (11.0 μL, 0.1 mmol). The reaction mixture was stirred at room temperature under an argon protection for 4 h. After removal of the solvent under a reduced pressure, the obtained crude product was chromatographed on silica gel flash column (300-400 mesh; eluent, PE:EA = 2:1) to give **SABC1** as a pale yellow solid (132 mg, 79%). HRMS (ESI) m/z calcd for $C_{26}H_{30}BNO_7$ $[M+Na]^+$: 502.2008; found 502.1998. ^{1}H NMR (400 MHz, $CDCl_3$) δ 8.81 (s, 1H), 8.45-8.36 (m, 1H), 7.84 (d, J = 6.8 Hz, 2H), 7.41 (d, J = 7.0 Hz, 2H), 6.62-6.55 (m, 1H), 6.43 (d, J = 19.9 Hz, 1H), 5.18 (s, 2H), 4.52-4.39 (m, 2H), 3.90 (t, J = 12.2 Hz, 2H), 3.82 (t, J = 6.2 Hz, 3H), 1.35 (s, 12H). ^{13}C NMR (100 MHz, $CDCl_3$) δ 165.8, 163.7, 160.6, 149.3, 138. 8, 135.3, 131.2, 126.3, 116., 114.30, 106.7, 99.6, 97.5, 84.0, 70.7, 67.7, 61.0, 55.7, 24.9.

SABC2 was prepared in a similar way as a yellow solid (149 mg, 86% yield). HRMS (ESI) m/z calcd for $C_{29}H_{30}BNO_6$ $[M+Na]^+$: 522.2058; found 522.2039. ^{1}H NMR (400 MHz, $CDCl_3$) δ 8.87 (d, J = 9.1 Hz, 1H), 7.89 (d, J = 9.1 Hz, 1H), 7.80 (dd, J = 15.7, 7.2 Hz, 3H), 7.75 (d, J = 8.4 Hz, 1H), 7.56 (t, J = 7.6 Hz, 1H), 7.41 (dd, J = 17.1, 7.6 Hz, 3H), 7.27 (d, J = 8.6 Hz, 1H), 5.39 (s, 2H), 4.61-4.41 (m, 2H), 4.12 (q, J = 7.1 Hz, 1H), 3.97 (s, 2H), 1.34 (s, 12H). ^{13}C NMR (100 MHz, $CDCl_3$) δ 162.5, 155.5, 152.2, 139.5, 135.2, 133.9, 131.7, 128.8, 128.7, 128.1, 126.4, 124.8, 123.5, 115.2, 115.1, 114.3, 109.6, 84.0, 71.2, 68.1, 60.9, 24.9.

SABC3 was prepared in a similar way as a yellow solid (149 mg, 85% yield). HRMS (ESI) m/z calcd for $C_{25}H_{28}BNO_6$ $[M+Na]^+$: 472.1907; found 472.1869. ^{1}H NMR (400 MHz, $CDCl_3$) δ 8.87 (s, 1H), 8.31 (d, J = 7.8 Hz, 1H), 7.84 (d, J = 7.9 Hz, 2H), 7.50-7.44 (m, 1H), 7.41 (d, J = 7.9 Hz, 2H), 7.07 (t, J = 7.6 Hz, 1H), 6.97 (d, J = 8.4 Hz, 1H), 5.20 (s, 2H), 4.46-4.41 (m, 2H), 3.96-3.91 (m, 2H), 1.35 (s, 12H). ^{13}C NMR (100 MHz, $CDCl_3$) δ 163.0, 158.4, 150.4, 139.0, 135.2, 135.2, 129.5, 126.3, 121.4, 121.1, 112.9, 101.8, 84.0, 70.7, 67.9, 60.9, 24.9.

Synthesis of Compounds CSU1-3. The mixture of compounds **3** (37 mg, 0.1 mmol), **SABC1** (48 mg, 0.1 mmol), EDCI (14.1 mg, 0.15 mmol), and DMAP (2.0 mg, 0.015 mmol) in dry CH_2Cl_2 (3.0 mL) was stirred at room temperature for 5 h. Then solvent was removed under a reduced pressure and the resultant solid was further purified by silica gel flash column (300-400 mesh; eluent, PE:EA = 5:1) to afford the desired product **CSU1** as a red solid (57 mg, 69%). HRMS (ESI) m/z calcd for $C_{46}H_{45}BN_2O_{10}S$ $[M+Na]^+$: 852.2780; found 852.2786. ^{1}H NMR (400 MHz, $CDCl_3$), δ 8.82 (s, 1H), 8.45-8.40 (m, 2H), 7.81 (d, J = 7.9 Hz, 2H), 7.38 (d, J = 7.9 Hz, 2H), 7.20 (s, 1H), 7.19-7.14 (m, 1H), 7.11-7.07 (m, 1H), 6.98 (t, J = 7.4 Hz, 1H), 6.91 (d, J = 8.2 Hz, 1H), 6.68 (s, 1H), 6.61 (dd, J = 8.9, 2.1 Hz, 1H), 6.45 (d, J = 2.2 Hz, 1H), 5.18 (s, 2H), 4.61 (s, 4H), 3.89-3.84 (m, 2H), 3.83 (s, 3H), 1.81 (dt, J = 14.9, 7.6 Hz, 2H), 1.47 (dd, J = 15.0, 7.4 Hz, 2H), 1.34 (s, 12H), 0.97 (t, J = 7.4 Hz, 3H). ^{13}C NMR (100 MHz, $CDCl_3$) δ 165.8, 163.3, 160.6, 157.0, 156.7, 151.1, 149.3, 148.3, 142.4, 138.8, 135.2, 131.3, 127.8, 127.5, 126.5, 126.2, 123.9, 123.2, 121.2, 116.6, 116.2, 114.4, 112.8, 112.7, 106.7, 102.1, 99.7, 97.8, 83.9, 70.7, 63.4, 62.7, 55.7, 48.3, 28.5, 24.9, 20.1, 13.7.

CSU2 was prepared in a similar procedure as a red solid (65 mg, 77%). HRMS (ESI) m/z calcd for $C_{49}H_{45}BN_2O_9S$ $[M+Na]^+$: 871.2752; found 871.2831. ^{1}H NMR (400 MHz, $CDCl_3$) δ 8.88 (s, 1H), 8.44 (s, 1H), 7.90 (d, J = 9.0 Hz, 1H), 7.79 (t, J = 8.5 Hz, 4H), 7.59-7.53 (m, 1H), 7.44 (d, J = 7.4 Hz, 3H), 7.28 (d, J = 5.2 Hz, 1H), 7.20-7.13 (m, 2H), 7.09 (d, J = 7.5 Hz, 1H), 6.98 (t, J = 7.4 Hz, 1H), 6.91 (d, J = 8.0 Hz, 1H), 6.67 (s, 1H), 5.40 (d, J = 8.8 Hz, 2H), 4.68 (s, 4H), 3.90–3.83 (m, 2H), 1.80 (d, J = 5.8 Hz, 2H), 1.49-1.43 (m, 2H), 1.33 (s, 12H), 0.97 (t, J = 7.2 Hz, 3H). ^{13}C NMR (100 MHz, $CDCl_3$) δ 162.2, 156.7, 154.9, 153.3, 152.2, 151.2, 149.7, 142.8, 140.4, 127.8, 126.5, 126.2, 125.6, 123.8, 121.9, 121.8, 116.1, 115.0, 114.2, 112.8, 102.5, 83.9, 71.1, 56.0, 48.1, 32.7, 26.1, 24.9, 20.1, 13.8.

CSU3 was prepared in a similar procedure as a red solid (50 mg, 61% yield). HRMS (ESI) m/z calcd for $C_{45}H_{43}BN_2O_9SNa$ $[M+Na]^+$: 821.2675; found 821.2587. ^{1}H NMR (400 MHz, $CDCl_3$) δ 8.90 (s, 1H), 8.43 (s, 1H), 8.34 (d, J = 7.9 Hz, 1H), 7.82 (d, J = 7.7 Hz, 2H), 7.47 (t, J = 7.5 Hz, 1H), 7.39 (d, J = 7.6 Hz, 2H), 7.23-7.14 (m, 2H), 7.08 (t, J = 8.6 Hz, 2H), 7.01-6.88 (m, 3H), 6.68 (s, 1H), 5.21 (s, 2H), 4.63 (s, 4H), 3.86 (t, J = 7.1 Hz, 2H), 1.80 (dd, J = 14.2, 7.3 Hz, 2H), 1.46 (dt, J = 14.0, 7.1 Hz, 2H), 1.34 (s, 12H), 0.97 (t, J = 7.3 Hz, 3H). ^{13}C NMR (100 MHz, $CDCl_3$) δ 162.7, 162.5, 156.7, 150.4, 148.4, 142.2, 139.0, 135.2, 129.5, 127.8, 127.5, 126.5, 126.2, 124.0, 123.0, 121.4, 121.0, 116.2, 113.0, 112.4, 102.0, 101.8, 99.9, 83.9, 70.6, 63.9, 62.6, 48.4, 28.4, 24.9, 20.1, 13.8.

Synthesis of Compound MC. Compound **MC** was synthesized for the mechanism study according to the literature method (Scheme 2).[45]

RESULTS AND DISCUSSION

Design and Synthesis of Probes CSU1-3. The rational design of the fluorescent probes is carried out by connecting a fused phenothiazine-based coumarin and a precursor of an-

other coumarin to form a single molecule **CSU1-3**, respectively (Scheme 1). The fused phenothiazine-based coumarin servers as a fluorophore as well as the chemoselective HClO oxidizable sulfide moiety; and a coumarin precursor is designed with boronate ester, a recognition group for H_2O_2.[46] It is expected that phenothiazine-based coumarin possesses a long wavelength emission, a relatively high quantum yield, a large stokes shift and good photo-stability.[47-49] HClO-mediated oxidation of the 'S' atom can significantly alternate the ICT (intramolecular charge transfer) effect and thereby resulting in a ratiometric fluorescence change from red to green (Scheme 2). The precursor of the coumarin carrying with a H_2O_2-sensitive boronate ester can be transferred into a blue-emitting *in situ* formed coumarin [50] in the presence of H_2O_2 through an oxidation-cyclization cascade process, releasing the phenothiazine-based coumarin at the same time. It's noteworthy that these three coumarins, phenothiazine-based coumarin and its oxidized derivative, the newly formed coumarin, shall have well-separated emissions to realize the ratiometric detection of HClO and H_2O_2 by a single molecule. With these considerations in mind, we designed three potential fluorescent probes differing in coumarin precursors, **CSU1-3**, and wish to obtain a bifunctional and dual-ratiometric fluorescent probe for HClO and H_2O_2.

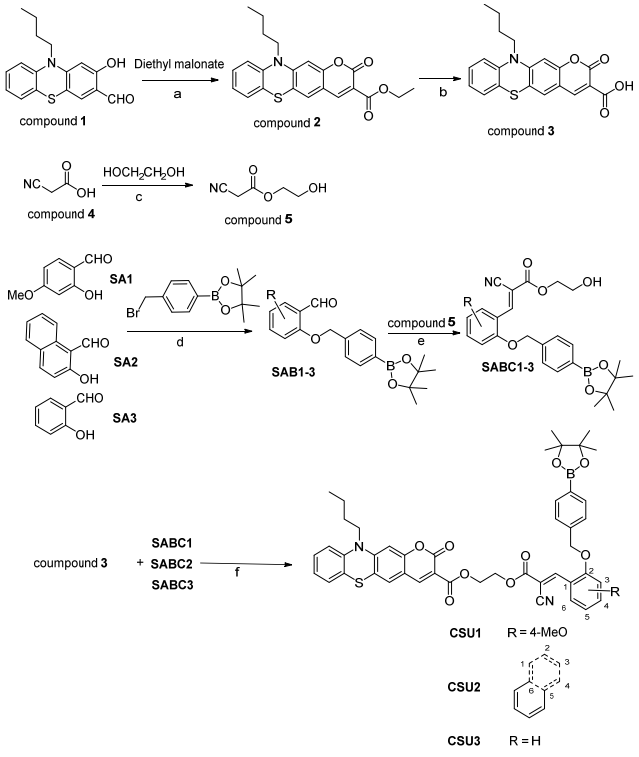

Scheme 1. Chemical structures and synthetic approaches to probes **CSU1-3**. (a) piperidine, CH_3CH_2OH, rt for 2 h, 63% yield; (b) NaOH, H_2O reflux for 1h, HCl, pH 3.0-4.0, 91% yield; (c) TsOH, toluene, 110 °C for 4 h, 56% yield; (d) K_2CO_3, CH_3CN, reflux for 5 h, 83-85% yield; (e) piperidine, CH_3CH_2OH, 25 °C for 4 h, 79-86% yield; (f) EDCI, DMAP, CH_2Cl_2, 25 °C for 5 h, 61-77% yield.

Taking probe **CSU1** as an example, it is expected that it emits a red signal (Scheme 2). HClO oxidizes the phenothiazine moiety to convert probe **CSU1** into **P1**, which makes a fluorescence change from red to green in a ratiometric manner.[44, 49] In contrast, the treatment of probe **CSU1** with H_2O_2 induces the formation of coumarin **MC** to turn on a new blue fluorescence while remaining the red fluorescence from compound **P2**. Such a change can offer a method to determine H_2O_2 in a ratiometric manner using the red fluorescence as a built-in standard. With respect to the co-existence of H_2O_2 and HClO, probe **CSU1** can undergo these two independent reactions to generate fluorophores **P3** and **MC** regardless of the addition order of H_2O_2 and HClO, which gives rise to mixed green and blue fluorescence signals at the same time. When adding H_2O_2 first, and then HClO to the solution of probe **CSU1**, a fluorescence colour change from red to red-blue and to green-blue, would be observed. In a reverse addition order (HClO first, and then H_2O_2), the phenomena would be red to green and to green-blue.

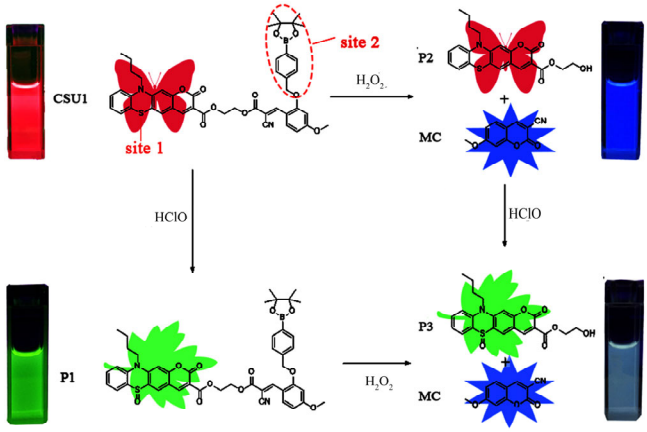

Scheme 2. The proposed sensing mechanism of probe **CSU1** for HClO, H_2O_2 and HClO/H_2O_2 with distinct fluorescence readouts.

Encouraged by the rational design strategy, we synthesized three probes, **CSU1-3** (Scheme 1) and their optical properties toward HClO and H_2O_2 were investigated in chemical and biological systems.

The synthesis of probes **CSU1-3** is described in Scheme 1. Phenothiazine-based salicylaldehyde (compound **1**) condenses with malonate and then undergoes a cyclization reaction to yield phenothiazine-based coumarin ester (compound **2**). Phenothiazine-based coumarin acid (compound **3**) is obtained *via* NaOH mediated saponification of compound **2** and subsequent acidification with dilute aqueous HCl solution. Cyanoacetic ester (compound **5**) is synthesized by a Fisher esterification of cyanoacetic acid (compound **4**). The synthesis of **SABC1-3** series can be achieved from corresponding salicylic aldehydes **SA1-3** *via* etherification and Knoevenagel condensation. Finally coupling of the two fragments **3** and **SABC1-3** in the presence of EDCI as coupling reagent delivers targets **CSU1-3**. These compounds are fully characterized by ^1H and ^{13}C NMR and HRMS with >95% purify for the study of their properties in chemical and biological systems.

Sensing Property of Probe CSU1. We took probe **CSU1** as a representative to thoroughly investigate its optical properties toward HClO or/and H_2O_2.

First, we performed the absorption spectra of probe **CSU1** in response to HClO and H_2O_2 in order to obtain appropriate excitation wavelength for fluorescence study. Probe **CSU1** exhibited two main absorption bands centred at 374 and 450 nm, respectively (Figure S1), which were characteristics of

phenothiazine-based coumarin and the precursor of another coumarin, respectively. In the presence of H_2O_2, the absorption band at 374 nm disappeared and a new 350 nm band occurred, suggesting the formation of new coumarin **MC**. The addition of HClO to the solution of probe **CSU1** resulted in the blue-shift in absorption from 450 nm to 384 nm, which was in agreement with the oxidation phenomenon of phenothiazine-based coumarin.

Second, we studied the fluorescence responses of probe **CSU1** to H_2O_2 and HClO, respectively (Figure 1). Probe **CSU1** itself exhibited a red fluorescence with a peak at 640 nm under the excitation at 440 nm, and was weakly fluorescent when excited at 376 nm. Upon the incremental addition of H_2O_2 to the solution of probe **CSU1**, the emission band at 640 nm remained stable under a 440 nm excitation, and a new blue emission band centred at 409 nm appeared under a 376 nm excitation and increasingly enhanced. To our delight, the intensity of red fluorescence from phenothiazine-based coumarin was nearly unchanged, which could serve as a built-in reference signal for probe **CSU1** to detect H_2O_2 through determining the ratio of fluorescence intensity at 409 nm and 640 nm ($I_{409\ nm}$ and $I_{640\ nm}$). It was seen in Figure 1C that the ratio of $I_{409\ nm}/I_{640\ nm}$ increased paralleling with H_2O_2 concentration. A linear relationship between the ratio of and the concentration of H_2O_2 (75.0-425.0 μM) was observed with a low detection limit of 15 nM. When HClO was added to the solution of probe **CSU1**, we observed: i) a decrease in the 640 nm emission peak and a new green emission band centred at 520 nm under a 440 nm excitation; and ii) only the green emission at 520 nm notably increased under a 376 nm excitation (Figure 1D). The fluorescence intensity ratio of I_{520}/I_{640} was linear to the concentration of HClO (Figure 1F) in the concentration range of 100.0-275.0 μM with a low detection limit (13 nM). It's noted that these three fluorescence signals (blue, green and red) for probe **CSU1** were well separated (over 110 nm difference), and thus avoiding the mutual interference in the detection H_2O_2 and HClO. As a consequence, probe **CSU1** could sensitively and selectively respond to H_2O_2 and HClO with distinct fluorescence signal patterns. The features of probe **CSU1** made it suitable for the simultaneous, qualitative and quantitative detection of H_2O_2 and HClO in a ratiometric manner.

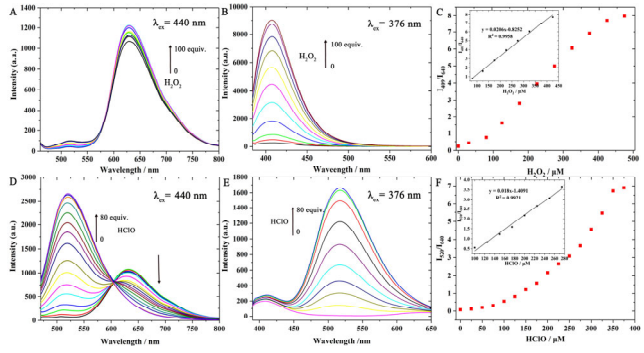

Figure 1 Fluorescence spectra of probe **CSU1** (5.0 μM) with the addition of different concentrations of H_2O_2 (0.0–100.0 equiv.) (A, B) and HClO (0.0–80.0 equiv.) (D, E) with the excitation at 440 nm and 376 nm, respectively. (C) The ratio of $I_{409\ nm}/I_{640\ nm}$ *vs* the concentration of H_2O_2, inset: the linear relationship between the ration of $I_{409\ nm}/I_{640\ nm}$ and the concentration of H_2O_2. (F) The ratio of $I_{520\ nm}/I_{640\ nm}$ *vs* the concentration of HClO, inset: the linear relationship between $I_{520\ nm}/I_{640\ nm}$ and the concentration of HClO.

Last, we explored probe **CSU1** to sense both H_2O_2 and HClO (Figure 2). The mixture of probe **CSU1** with H_2O_2 exhibited two kinds of fluorescence signals: red with λ_{max} = 640 nm (λ_{ex} = 440 nm) and blue with λ_{max} = 409 nm (λ_{ex} = 376 nm), while the mixture of probe **CSU1** with HClO only showed green fluorescence with λ_{max} = 520 (λ_{ex} = 376 nm). The successive addition of H_2O_2 and HClO to the solution of probe **CSU1** resulted in a mixed blue and green fluorescence signals (376 nm excitation). The same result was obtained when probe **CSU1** was treated with these two species in a reverse order. It's noted that both of H_2O_2 and HClO could be detected quantitatively regardless of the addition order. For example, in the addition order of H_2O_2 and HClO, the ratio of $I_{520\ nm}/I_{409\ nm}$ exhibited a good linear relationship with concentration of HClO in a range of 100.0-275.0 μM. The ratio of $I_{409\ nm}/I_{520\ nm}$ was linear with the concentration of H_2O_2 (75.0-425.0 μM) when the addition order was HClO and H_2O_2. These results clearly demonstrated that probe **CSU1** could simultaneously detect H_2O_2 and HClO through the dual-emission detection without interference from the presence of each other.

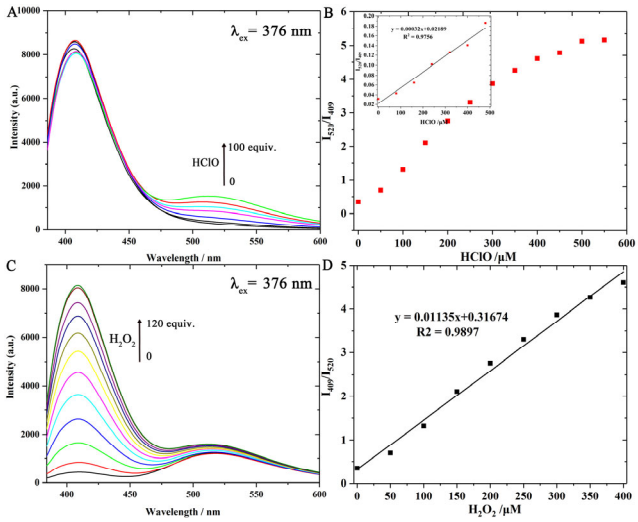

Figure 2. Fluorescence spectra (A) and fluorescence intensity raitio ($I_{520\ nm}/I_{409\ nm}$) (B) of probe **CSU1** (5.0 μM) treated with 100.0 equiv. H_2O_2 and then incubated with various amounts of HClO (0.0-100.0 equiv.). Fluorescence spectra (C) and fluorescence intensity ratio ($I_{409\ nm}/I_{520\ nm}$) (D) of probe **CSU1** (5.0 μM) treated with 80.0 equiv. HClO and then incubated with various amounts of H_2O_2 (0.0 -120.0 equiv.). Inset (B): the linear relationship between $I_{409\ nm}/I_{520\ nm}$ and the concentration of HClO. Excitation wavelength: 376 nm.

Sensing Property of Probe CSU2. We then investigated the spectral properties of probe **CSU2** in response to H_2O_2 and HClO (shown in Figure S7). In the presence of H_2O_2, the blue fluorescence at 450 nm (λ_{ex} = 403 nm) increased while the red fluorescence at 640 nm (λ_{ex} = 440 nm) remained unchanged (Figures S7A and S7B), which was quite similar to the fluorescence performance of probe **CSU1**. The new blue-emitting coumarin **HC**, was isolated from the reaction mixture and was validated by TLC, optical and HRMS analysis (Figures S8, S9, S40 and S41). With the addition of HClO, the fluorescence of probe **CSU2** at 640 nm gradually disappeared, and a new green fluorescence occurred when excited at 440 nm (Figure S7E). Unexpectedly, under a 403 nm excitation, the blue fluorescence at 450 nm was also observed in the solution of probe **CSU2** with HClO, indicating the formation of the new

coumarin, a cyclization product (Figure S7D). This result suggested HClO could oxidize both phenoxazine moiety and cleave the borate ether bond as well.[51] The successive addition of H_2O_2 and then HClO to the solution of probe **CSU2** still induced a fluorescence color change from red to blue-red, and finally to blue-green (Figure S7C). In a reverse addition order of HClO and then H_2O_2, however, fluorescence color first changed from red to blue-green toward HClO and remained unchanged with the further addition of H_2O_2 because both of the recognition sites were sensitive to HClO (Figure S7E). As a result, probe **CSU2** could still detect H_2O_2 and HClO individually: red to blue-red fluorescence change for H_2O_2, and red to blue-green fluorescence change for HClO, but was unable to sense H_2O_2 and HClO successively both in forward and reverse addition orders.

Sensing Property of Probe CSU3. Finally, we investigated the optical properties of probe **CSU3** in a similar manner. As shown in Figure S10, the addition of H_2O_2 to the solution of probe **CSU3** didn't affect the red fluorescence at 640 nm (λ_{ex} = 440 nm), and resulted in an 8-fold enhancement of the blue fluorescence at 420 nm (λ_{ex} = 340 nm) (Figures S10A and S10B). The response of probe **CSU3** towards HClO was similar to that of probe **CSU1** (Figures S10D and S10E), inducing a red to green fluorescence change. Thus, probe **CSU3** could also selectively detect HClO and H_2O_2 individually. Considering the low fluorescence quantum yield of the new formed blue-emitting coumarin, 2-oxo-2H-chromene-3-carbonitrile, ($\Phi_f < 0.01$)[52], probe **CSU3** was not the ideal fluorescent probe.

The above screening studies of probes **CSU1-3** indicated that probe **CSU1** exhibited the best performance. Hence, we chose it for following studies.

Mechanistic Studies. Probe **CSU1** consists of two sensing segments: **SABC1** and compound **2** (Scheme 1). It is expected that **SABC1** derived segment would react with H_2O_2 to form a blue fluorescent coumarin, **MC**, while compound **2** would response to HClO to form the green fluorescent phenothiazine-based coumarin. To confirm the sensing mechanism of probe **CSU1** to H_2O_2, the optical properties of the expected product **MC** and the mixture of **SABC1** and H_2O_2 were investigated. It was shown in Figure S2 that **MC** and the mixture **SABC1** with H_2O_2 had nearly identical absorption and fluorescence spectra. Meanwhile, the fluorescence response of compound **2** toward HClO was studied to prove the reaction between probe **CSU1** and HClO. Compound **2** displayed a fluorescence change from red to green in response to HClO (Figure S3), which was similar to the fluorescence behavior of probe **CSU1** before and after the treatment of HClO (Figure 1D). To obtain more concrete evidence for the sensing mechanism, mass spectral analysis was performed on probe **CSU1** (Figures S28-S30). As shown in Figure S28, the reaction mixture of probe **CSU1** with HClO had a mass peak at m/z = 867.2746, which well matched the exact molecular mass of the anticipated compound **P1** ($[M+Na]^+$ = 867.2729) (Scheme 1). For the case of probe **CSU1** reacting with H_2O_2, two peaks at m/z = 434.1033 and 224.0320 were found, which corresponded to the expected compounds **P2** and **MC**, respectively (Figure S29). Moreover, the HR-MS spectrum of probe **CSU1** with the addition of H_2O_2 and HClO in both the forward and reverse reaction orders gave two mass peaks at 450.1000 and 224.0320, corresponding to the expected compounds **P3** and **MC**, respectively (Figure S30). The above results clearly supported the working hypotheses, as illustrated in Scheme 1.

Selectivity and Kinetic Studies. To verify the selectivity of probe **CSU1** towards H_2O_2 and HClO over other related ROS, probe **CSU1** was incubated with various biologically relevant species including NO, $ONOO^-$, $^{\bullet}OH$, $^1O_2$, $O_2^{-\bullet}$, $ROO^{\bullet}$, *t*-$BuO^{\bullet}$. The fluorescence signals were collected through different color channels. As seen in Figure 3A, under the excitation of 376 nm, only H_2O_2 induced a remarkable fluorescence enhancement at 409 nm (40-folds) while other analytes hardly caused fluorescence intensity changes even within a 100 min incubation time. Similarly, under a 440 nm excitation, only HClO resulted in a fluorescence enhancement at 520 nm and a decline at 640 nm, while negligible fluorescence changes were observed on the two emission bands for other test species (Figure 3B). These experimental results demonstrated that probe **CSU1** could be used to selectively detect H_2O_2 and HClO in a ratiometric pattern.

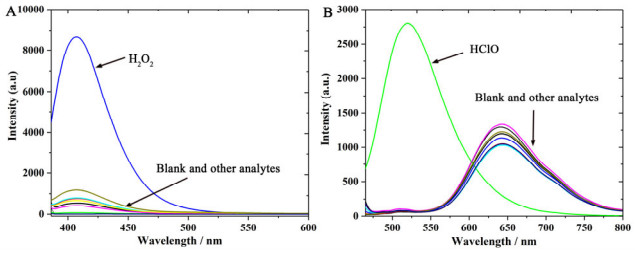

Figure 3. (A) Fluorescence spectra of probe **CSU1** (5.0 μM) in the presence of H_2O_2 (500.0 μM) and various interfering analytes (500.0 μM), excited at 376 nm; (B) Fluorescence spectra of probe **CSU1** (5.0 μM) in the presence of HClO (400.0 μM) and the interfering analytes (400.0 μM), excited at 440 nm. The interfering analytes include NO, $ONOO^-$, $^{\bullet}OH$, $^1O_2$, $O_2^{-\bullet}$, $ROO^{\bullet}$ and *t*-$BuO^{\bullet}$.

pH Effect. In order to investigate whether probe **CSU1** is capable of sensing H_2O_2 and HClO under physiological conditions, we then studied pH effect on the fluorescence performance of this probe. As shown in Figures S11 and S12, the fluorescence behavior of probe **CSU1** remained unchanged within a wide pH range. In the presence of HClO, the probe showed a striking enhancement in fluorescence ratio (I_{520}/I_{640}) between pH 6.0 to 10.0. The mixture of H_2O_2 with probe **CSU1** exhibited a large ratio of fluorescence intensities at 409 nm and 640 nm (I_{409}/I_{640}) between pH 6.0 to 10.0. These results indicated that probe **CSU1** has an excellent stability and exhibits a good performance to sense HClO and H_2O_2 in physiological environments.

***In Situ* Monitoring of HClO Produced from H_2O_2 and Cl^- in Solution.** It's known that HClO can be endogenously produced from the reaction of chloride ion with H_2O_2 catalysed by MPO in biological systems. Thus, we used probe **CSU1** to investigate the above process *in vitro*. As illustrated in Figure 4A, when H_2O_2 was added into the MPO/**CSU1**/Cl^- system, the fluorescence at 409 nm (λ_{ex} = 390 nm) rose rapidly in the beginning and reached a plateau within 15 min. At the same time, the fluorescence at 520 nm (λ_{ex} = 390 nm) occurred and significantly increased, suggesting the generation of HClO in the MPO-catalysed process. However, the addition of H_2O_2 to the **CSU1**/Cl^- system without MPO did not induce any fluorescence at 520 nm, and only resulted in a fluorescence enhancement at 409 nm (Figure 4B). These results showed probe **CSU1** was capable of monitoring the *in-situ* generation of HClO from MPO/H_2O_2/Cl^- system.

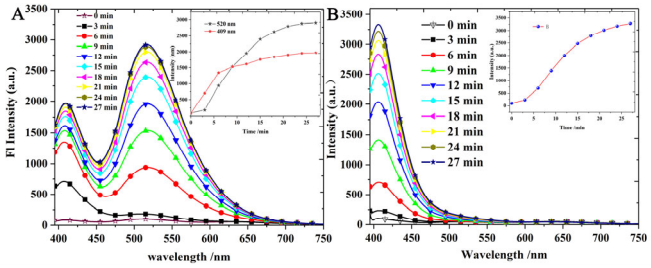

Figure 4. (A) Time-dependent fluorescence of probe **CSU1** (5.0μM) in MPO/H_2O_2/Cl^- system (500.0μM H_2O_2, 0.5 U/mL MPO, 2.0 mM NaCl). (B) Time-dependent fluorescence of probe **CSU1** (5.0 μM) in H_2O_2/Cl^- system (500.0 μM H_2O_2, 2.0 mM NaCl). Excitation wavelength: 390 nm.

Fluorescence Imaging of H_2O_2 and HClO in Living Cells. Encouraged by the favourable properties of probe **CSU1** in detecting of H_2O_2 and HClO *in vitro*, we determined to assess its capability to image intracellular H_2O_2 and HClO. The cytotoxicity of probe **CSU1** was tested by the MTT assay using MCF-7 cells and it was found that **CSU1** had a low toxicity (Figure S15). We collected the fluorescence signals in living cells from three channels to detect H_2O_2 and HClO. Cells gave off strong fluorescence in the red channel (570-650 nm) when only treated with probe **CSU1** (Figure 5d). When **CSU1**-treated cells were further incubated with HClO, a strong fluorescence in the green channel (515-580 nm) was seen from inside cells (Figure 5h). As expected, we observed strong fluorescent signals in both blue (420-500 nm) and red (570-650 nm) channels upon the incubation of **CSU1**-treated cells with H_2O_2 (Figures 5l and 5n). We then further tested the fluorescence behaviour of probe **CSU1** in imaging intracellular H_2O_2 and HClO in living cells in different addition orders. Cells were successively stained with probe **CSU1** for 20 min, HClO for 20 min and H_2O_2 for another 1 h, and bright fluorescence signals appeared from both blue and green channels (Figures 5q and 5r). In the imaging experiment with a reverse addition order of these two analytes, same results were observed (Figures 5v and 5w). These results demonstrated that probe **CSU1** could selectively image intracellular H_2O_2 and/or HClO through three different channels.

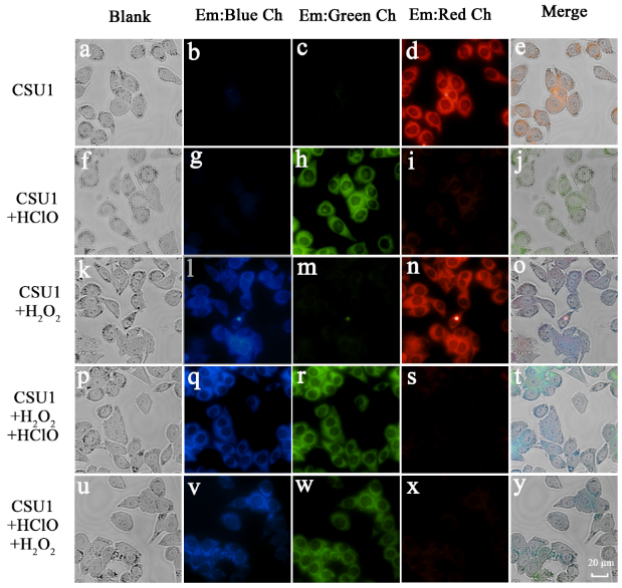

Figure 5. Bright and fluorescence images of living MCF-7 cells. (a-e) Cells only treated with probe **CSU1** (5.0 μM) for 20 min. (f-j) Cells incubated with probe **CSU1** (5.0 μM) for 20 min and then treated with HClO (400.0 μM) for another 20 min. (k-o) Cells incubated with probe **CSU1** (5.0 μM) for 20 min and then treated with H_2O_2 (500.0 μM) for another 1 h. (p-t) Cells treated with probe **CSU1** (5.0 μM) for 20 min, incubated with H_2O_2 (500.0 μM) for 1 h, and further loaded with HClO (400.0 μM) for 20 min. (u-y) Cells treated with probe **CSU1** (5.0 μM) for 20 min, incubated with HClO (400.0 μM) for 20 min, and further loaded with H_2O_2 (500.0 μM) for 1 h. Blue channel: 420-500 nm (excited at 355-385 nm). Green channel: 515-580 nm (excited at 390-420 nm). Red channel: 570-650 nm (excited at 435-460 nm). Scale bar: 20 μm.

Fluorescence Imaging of Intracellular HClO Produced by MPO System. Finally, we monitored the endogenous HClO generation from H_2O_2 and Cl^- in the presence of MPO enzyme in living cells. The treatment of MCF-7 cells with probe **CSU1** and NaCl only triggered strong fluorescence signals in the red channel (Figures 6a-6e). When cells were treated with probe **CSU1**, H_2O_2 and NaCl, bright fluorescence emerged in both the blue and red channels (Figures 6f-6j). When cells were pretreated with probe **CSU1**, NaCl and MPO, and then incubated with H_2O_2, strong fluorescence signals in the green channel, moderate fluorescence in the blue channel and very weak signals in the red channel were observed (Figures 6k-6o).

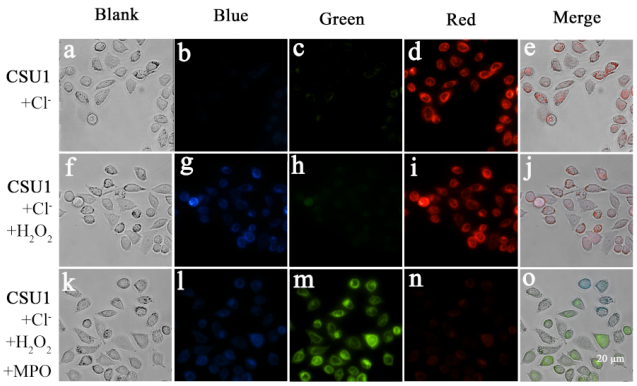

Figure 6. Bright and fluorescence images of living MCF-7 cells. (a-e) Cells incubated with probe **CSU1** (5.0 μM) and NaCl (2.0 mM) for 20 min. (f-j) Cells incubated with probe **CSU1** (5.0 μM) and NaCl (2.0 mM) for 20 min and then treated with H_2O_2 (500.0 μM) for another 30 min. (k-o) Cells incubated with **CSU1** (5 μM), NaCl (2.0 mM) and MPO (0.5 U/mL) for 20 min, and further treated with H_2O_2 (500.0 μM) for 30 min. Blue channel: 420-500 nm (excited at 355-385 nm). Green channel: 515-580 nm (excited at 390-420 nm). Red channel: 570-650 nm (excited at 435-460 nm). Scale bar: 20 μm.

Lastly, probe **CSU1** was used to monitor the real-time endogenous generation of HClO from H_2O_2 and Cl^- in the presence of MPO enzyme in living cells. As shown in Figure 7 and the dynamic video (seen in SI), the original bright red fluorescence from cells treated with probe **CSU1**, NaCl and MPO gradually decreased after the addition of H_2O_2. At the same time, green fluorescence occurred and was enhanced in a time-dependent manner. These experiments clearly indicated the fast generation of endogenous HClO from MPO/H_2O_2/Cl^- system in living cells.

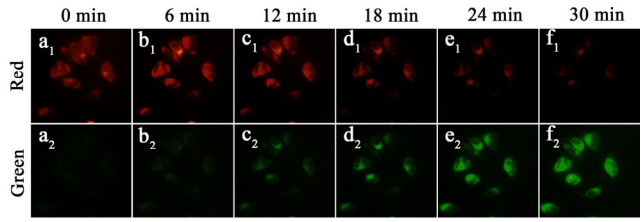

Figure 7. Real-time fluorescence images of MCF-7 cells (pretreated with Cl^- and MPO) in the red and green channels, respectively, at 0, 6, 12, 18, 24, 30 min after the addition of H_2O_2. Red channel: 570-650 nm (excited at 435-460 nm). Green channel: 515-580 nm (excited at 390-420 nm). Scale bar: 20 μm.

CONCLUSION

In summary, a new dual-ratiometric fluorescent probe has been built for simultaneously detecting HClO and H_2O_2 in solution and living cells for the first time. This probe displays high selectivity and sensitivity for H_2O_2 and HClO. Furthermore, this probe has been successfully used to image H_2O_2 and HClO in living cells using different fluorescence signal combinations. Importantly, it can be applied to monitor the process of endogenous generation of HClO from H_2O_2/Cl^-/MPO system. It is expected that the probe holds a geat potential as a useful tool for biomedical scientists to investigate and dissect the correlation of HClO and H_2O_2 engaged biological processes in physiological and pathological conditions.

ASSOCIATED CONTENT

Supporting Information

Chemical structures of compounds, additional optical spectral data, ^1H NMR, ^{13}C NMR and HRMS spectra of compounds. The Supporting Information is available free of charge via the Internet at http://pubs.acs.org.

AUTHOR INFORMATION

Corresponding Authors

* Fax: +86-731-88836954; Tel: +86-731-88836954; E-mail: xzsong@csu.edu.cn.
* Fax: +1-520-626-2466; Tel: +1-520-626-1764; E-mail: wwang@pharmacy.arizona.edu.

Notes

The authors declare no competing financial interest.

ACKNOWLEDGMENT

This work was supported by the National Natural Science Foundation of China (No. U1608222), the State Key Laboratory of Fine Chemicals (KF1606), the State Key Laboratory of Chemo/Biosensing and Chemometrics (2016005) and the Fundamental Research Funds for the Central Universities of Central South University (No. 202045010).

REFERENCE

(1) Pelicano, H.; Carney, D.; Huang, P. ROS stress in cancer cells and therapeutic implications. *Drug Resist. Updates* **2004**, 7(2), 97-110.
(2) Chen, X.; Wang, F.; Hyun, J. Y.; Wei, T.; Qiang, J.; Ren, X.; Shin, I.; Yoon, J. Recent progress in the development of fluorescent, luminescent and colorimetric probes for detection of reactive oxygen and nitrogen species. *Chem. Soc. Rev.* **2016**, 45(10), 2976-3016.
(3) Giorgio, M.; Trinei, M.; Migliaccio, E.; Pelicci, P. G. Hydrogen peroxide: a metabolic by-product or a common mediator of ageing signals? *Nat. Rev. Mol. Cell Biol.* **2007**, 8(9), 722-728.
(4) Winterbourn, C. C. Reconciling the chemistry and biology of reactive oxygen species. *Nat. Chem. Biol.* **2008**, 4(5), 278-286.
(5) Forman, H. J. Ann. N. Y. Reactive oxygen species and α, β-unsaturated aldehydes as second messengers in signal transduction. *Acad. Sci.* **2010**, 1203 (1), 35-44.
(6) Sauer, H.; Wartenberg, M.; Hescheler, J. Reactive oxygen species as intracellular messengers during cell growth and differentiation. *Cell. Physiol. Biochem.* **2001**, 11(4), 173-186.
(7) Rhee, S. G. H_2O_2, a necessary evil for cell signaling. *Science* **2006**, 312(5782), 1882-1883.
(8) Stone, J. R.; Yang, S. Hydrogen peroxide: a signaling messenger. *Antioxid. Redox Signal.* **2006**, 8(4-4), 243-270.
(9) Noh, J.; Kwon, B.; Han, E.; Park, M.; Yang, W.; Cho, W.; Yoo, W.; Khang, G.; Lee, D. Amplification of oxidative stress by a dual stimuli-responsive hybrid drug enhances cancer cell death. *Nat. Commun.*, **2015**, 6, 6907-6915.
(10) Faria, A.; Persaud, S. J. Cardiac oxidative stress in diabetes: Mechanisms and therapeutic potential. *Pharmacol. Ther.*, **2017**, 172, 50-62.
(11) Wei, H.; Shang, T.; Wu, T.; Liu, G.; Ding, L.; Liu, X. Construction of an ultrasensitive non-enzymatic sensor to investigate the dynamic process of superoxide anion release from living cells. *Biosens. Bioelectron.* **2018**, 100, 8-15.
(12) Nathan, C.; Cunningham-Bussel, A. Beyond oxidative stress: an immunologist's guide to reactive oxygen species. *Nat. Rev. Immunol.* **2013**, 13(5), 349-361.
(13) Pussard, E.; Chaouch, A.; Said, T. Radioimmunoassay of free plasma metanephrines for the diagnosis of catecholamine-producing tumors. *Clin. Chem. Lab. Med.* **2014**, 52(3), 437-444.
(14) Barnham, K. J.; Masters, C. L.; Bush, A. I. Neurodegenerative diseases and oxidative stress. *Nat. Rev. Drug Discovery* **2004**, 3, 205-214.
(15) Lin, M. T.; Beal, M. F. Alzheimer's APP mangles mitochondria. *Nat. Med.* **2006**, 12(11), 1241-1243.
(16) Shah, A. M.; Channon, K. M. Free radicals and redox signalling in cardiovascular disease. *Heart* **2004**, 90(5), 486-487.
(17) Yue, Y.; Huo, F.; Yin, C.; Escobedo, J. O.; Strongin, R. M. Recent progress in chromogenic and fluorogenic chemosensors for hypochlorous acid. *Analyst* **2016**, 141(6), 1859-1873.
(18) Whiteman, M.; Cheung, N. S.; Zhu, Y.-Z.; Chu, S. H.; Siau, J. L.; Wong, B. S.; Armstrong, J. S.; Moore, P. K. Hydrogen sulphide: a novel inhibitor of hypochlorous acid-mediated oxidative damage in the brain? *Biochem. Biophys. Res. Commun.* **2005**, 326(4), 794-798.
(19) Pattison, D. I.; Davies, M. J. Kinetic analysis of the reactions of hypobromous acid with protein components: implications for cellular damage and use of 3-bromotyrosine as a marker of oxidative stress. *Biochem.* **2004**, 43(16), 4799-4809.
(20) Li, G.; Lin, Q.; Sun, L.; Feng, C.; Zhang, P.; Yu, B.; Chen, Y.; Wen, Y.; Wang, H.; Ji, L.; Chao, H. A mitochondrial targeted two-photon iridium (III) phosphorescent probe for selective detection of hypochlorite in live cells and in vivo. *Biomater.* **2015**, 53, 285-295.
(21) Pattison, D. I.; Hawkins, C. L.; Davies, M. J. Hypochlorous acid-mediated oxidation of lipid components and antioxidants present in low-density lipoproteins: absolute rate constants, product analysis, and computational modeling. *Chem. Res. Toxicol.* **2003**, 16(4), 439-449.
(22) Li, H.; Cao, Z.; Ray Moore, D.; Jackson, P.; Barnes, S.; Lambeth, J.; J Thannickal, V.; Cheng, G. Microbicidal activity of vascular peroxidase 1 in human plasma via generation of hypochlorous acid. *Infect. Immun.* **2012**, 80(7), 2528-2537.
(23) Hawkins, C. L.; Pattison, D. I.; Davies, M. J. Hypochlorite-induced oxidation of amino acids, peptides and proteins. *Amino Acids* **2003**, 25(3-4), 259-274.
(24) Yap, Y. W.; Whiteman, M.; Cheung, N. S. Chlorinative stress: an under appreciated mediator of neurodegeneration? *Cell. Signal.* **2007**, 19(19), 219-228.
(25) Klebanoff, S. J. Myeloperoxidase: friend and foe. *J. Leukocyte Biol.* **2005**, 77(5), 598-625.
(26) Henrique de Araujo, T.; Okada, S. S.; Ghosn, E. E. B.; Taniwaki, N. N.; Rodrigues, M. R.; Rogerio de Almeida, S.; Mortara, R. A.; Russo, M.; Campa, A.; Albuquerque, R. C. Intracellular localization

of myeloperoxidase in murine peritoneal B-lymphocytes and macrophages. *Cell. Immunol.* **2013**, 281(1), 27-30.
(27) Davies, M. J. Myeloperoxidase-derived oxidation: mechanisms of biological damage and its prevention. *J. Clin. Biochem. Nutr.* **2010**, 48(1), 8-19.
(28) Barnham, K. J.; Masters, C. L.; Bush, A. I. Neurodegenerative diseases and oxidative stress. *Nat. Rev. Drug Discovery* **2004**, 3(3), 205-214.
(29) Park, L.; Zhou, P.; Pitstick, R.; Capone, C.; Anrather, J.; Norris, E. H.; Younkin, L.; Younkin, S.; Carlson, G.; McEwen, B. S.; Iadecola, C. Nox2-derived radicals contribute to neurovascular and behavioral dysfunction in mice overexpressing the amyloid precursor protein. *Proc. Natl. Acad. Sci.* **2008**, 105(4), 1347.
(30) Chen, X.; Tian, X.; Shin, I.; Yoon, J. Fluorescent and luminescent probes for detection of reactive oxygen and nitrogen species. *Chem. Soc. Rev.* **2011**, 40(9), 4783-4804.
(31) Giepmans, B. N. G.; Adams, S. R.; Ellisman, M. H.; Tsien, R. Y. The fluorescent toolbox for assessing protein location and function. *Science.* **2006**, 312(5771), 217.
(32) Xiao, H.; Li, P., Hu, X.; Shi, X.; Zhang, W.; Tang, B. Simultaneous fluorescence imaging of hydrogen peroxide in mitochondria and endoplasmic reticulum during apoptosis. *Chem. Sci.* **2016**, 7(9), 6153-6159.
(33) Duan, C.; Won, M.; Verwilst, P.; Xu, J.; Kim, H. S.; Zeng, L.; Kim, J. S. In vivo imaging of endogenously produced HClO in zebrafish and mice using a bright, photostable ratiometric fluorescent probe. *Anal. Chem.* **2019**, 91(6), 4172-4178.
(34) Gao, C.; Tian, Y.; Zhang, R. Jing, J.; Zhang, X. Endoplasmic reticulum-directed ratiometric fluorescent probe for quantitive detection of basal H_2O_2. *Anal. Chem.* **2017**, 89(23), 12945-12950.
(35) Ren, M.; Deng, B.; Zhou, K.; Kong, X.; Wang, J.-Y.; Lin, W. Single fluorescent probe for dual-Imaging viscosity and H_2O_2 in mitochondria with different fluorescence signals in living cells. *Anal. Chem.* **2017**, 89(1), 552-555.
(36) Shu, W.; Yan, L.; Liu, J.; Wang, Z.; Zhang, S.; Tang, C.; Liu, C.; Zhu, B.; Du, B. Highly selective fluorescent probe for the sensitive detection of inorganic and organic mercury species assisted by H_2O_2. *Ind. Eng. Chem. Res.* **2015**, 54(33), 8056-8062.
(37) Wu, W.; Li, J., Chen, L.; Ma, Z.; Zhang, W.; Liu, Z.; Cheng, Y.; Du, L.; Li, M. Bioluminescent probe for hydrogen peroxide imaging in vitro and in vivo. *Anal. Chem.* **2014**, 86(19), 9800-9806.
(38) Zhang, W.; Liu, W.; Li, P., Huang, F.; Wang, H.; Tang, B. Rapid-response fluorescent probe for hydrogen peroxide in living cells based on increased polarity of C–B bonds. *Anal. Chem.* **2015**, 87(19), 9825-9828.
(39) Giorgio, M.; Trinei, M.; Migliaccio, E.; Pelicci, P. G. Hydrogen peroxide: a metabolic by-product or a common mediator of ageing signals? *Nat. Rev. Mol. Cell Biol.* **2007**, 8(9), 722.
(40) Dickinson, B. C.; Srikun, D.; Chang, C. J. Mitochondrial-targeted fluorescent probes for reactive oxygen species. *Curr. Opin. Chem. Biol.* **2010**, 14(11), 50-56.
(41) Xiong, H.; He, L.; Zhang, Y.; Wang, J.; Song, X.; Yang, Z. A ratiometric fluorescent probe for the detection of hypochlorous acid in living cells and zebra fish with a long wavelength emission. *Chin. Chem. Lett.* **2019**, 30(1), 1075-1077.
(42) Gudipudi, G.; Sagurthi, S. R.; Perugu, S.; Achaiah, G.; Krupadanam, G. D. α-Glucosidase inhibitory activity, molecular docking, QSAR and ADMET properties of novel 2-aminophenyldiazenyl-4H-chromene derivatives. *RSC Adv.* **2014**, 4(12), 56489-56501.
(43) Hao, W. H.; Yan, P.; Li, G.; Wang, Z. Y. Short-conjugated zwitterionic cyanopyridinium chromophores: synthesis, crystal structure, and linear/nonlinear optical properties. *Dyes Pigm.* **2014**, 111, 145-155.
(44) Cao, D.; Peng, J.; Hong, Y.; Fang, X.; Wang, L.; Meier, H. Enhanced performance of the dye-sensitized solar cells with phenothiazine-based dyes containing double D−A branches. *Org. Lett.* **2011**, 13(7), 1610-1613.
(45) Fringuelli F.; Piermatti O.; Pizzo F. One-pot synthesis of 3-carboxycoumarins via consecutive Knoevenagel and Pinner reactions in water. *Synth*. **2003**, 15, 2331-2334.
(46) Yuan, L.; Lin, W. Y.; Xie, Y. N. Chen, B.; Zhu, S. S. Single Fluorescent probe responds to H_2O_2, NO, and H_2O_2/NO with three different sets of fluorescence signals. *J. Am. Chem. Soc.* **2012**, 134 (2), 1305-1315.
(47) Kazlauskas, K.; Mikulėnaitė, J.; Karpicz, R.; Gulbinas, V.; Simokaitiene, J.; Michaleviciute, A.; Keruckas, J.; Grazulevicius, J. V. Photostability of phenothiazinyl-substituted ethylenes. *Dyes Pigm.* **2009**, 83(2), 168-173.
(48) Găină, L.; Torje, I.; Gal, E.; Lupan, A.; Bischin, C.; Silaghi-Dumitrescu, R.; Damian, G.; Lönnecke, P.; Cristea, C.; Silaghi-Dumitrescu, L. Microwave assisted synthesis, photophysical and redox properties of (phenothiazinyl) vinyl-pyridinium dyes. *Dyes Pigm.* **2014**, 102, 315-325.
(49) Xiao, H.; Xin, K.; Dou, H.; Yin, G.; Quan, Y.; Wang, R. A fast-responsive mitochondria-targeted fluorescent probe detecting endogenous hypochlorite in living RAW 264.7 cells and nude mouse. *Chem. Commun.* **2015**, 51(8), 1442-1445.
(50) Qi, F. P.; Zhang, Y.; Wang, B. H.; Chen, W. Q.; Yang, L.; Yang, Z. G.; Song, X. Z. A fluorescent probe for the dicriminatory detecion of Cys/Hcy, GSH and H_2S in living cells and zebrafish. *Sens. Actuators, B Chem.* **2019**, 296, 126533.
(51) Shu, W.; Yan, L.; Wang, Z.; Liu, J.; Zhang, S.; Liu, C.; Zhu, B. A novel visual and far-red fluorescent dual-channel probe for the rapid and sensitive detection of hypochlorite in aqueous solution and living cells. *Sens. Actuators, B Chem.* **2015**, 221, 1130-1136.
(52) Rabahi, A.; Makhloufi-Chebli, M.; Hamdi, S. M.; Silva, A. M. S.; Kheffache, D.; Boutemeur-Kheddis, B.; Hamdi, M. Synthesis and optical properties of coumarins and iminocoumarins: Estimation of ground and excited-state dipole moments from a solvatochromic shift and theoretical methods. *J. Mol. Liq.* **2014**, 195, 240-247.

TOC

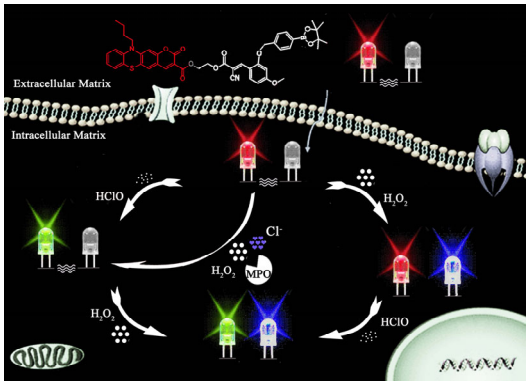
Extracellular Matrix
Intracellular Matrix
HClO
H_2O_2
Cl^-
H_2O_2
MPO
H_2O_2
HClO